Published in final edited form as:
Neurochem Res. 2011 May ; 36(5): 819–828. doi:10.1007/s11064-011-0409-2.

Neurodegenerative Effects of Recombinant HIV-1 Tat(1-86) are Associated with Inhibition of Microtubule Formation and Oxidative Stress-Related Reductions in Microtubule-Associated Protein-2(a,b)

Tracy R. Butler, **Katherine J. Smith**, **Rachel L. Self**, **Brittany B. Braden**, and **Mark A. Prendergast**
Department of Psychology, University of Kentucky, B449 Biomedical and Biological Sciences Research Building, 741 South Limestone St., Lexington, KY 40536-0509, USA

Mark A. Prendergast: prender@email.uky.edu

Abstract

The human immunodeficiency virus 1 (HIV-1) protein Trans-activator of Transcription (Tat) is a nuclear regulatory protein that may contribute to the development of HIV-1 associated dementia by disrupting the neuronal cytoskeleton. The present studies examined effects of recombinant Tat(1-86; 1–100 nM) on microtubule-associated protein (MAP)-dependent and MAP-independent microtubule formation ex vivo and oxidative neuronal injury in rat organotypic hippocampal explants. Acute exposure to Tat(1-86) (≥1 nM) markedly reduced MAP-dependent and –independent microtubule formation ex vivo, as did vincristine sulfate (0.1–10 μM). Cytotoxicity, as measured by propidium iodide uptake, was observed in granule cells of the DG with exposure to 100 nM Tat(1-86) for 24 or 72 h, while significant reductions in MAP-2 immunoreactivity were observed in granule cells and pyramidal cells of the CA1 and CA3 regions at each timepoint. These effects were prevented by co-exposure to the soluble vitamin E analog Trolox (500 μM). Thus, effects of Tat(1-86) on the neuronal viability may be associated with direct interactions with microtubules and generation of oxidative stress.

Keywords

Acquired immune deficiency syndrome; Neurotoxicity; Trolox; Tubulin

Introduction

Human immunodeficiency virus type-1 (HIV-1) is associated with cognitive dysfunction and neurodegeneration of many cortical and subcortical regions. HIV-associated neurocognitive disorder (HAND) encompasses varying severities of cognitive dysfunction, ranging from mild cognitive decline to impairment in all aspects of daily living [47]. Structural abnormalities of many cortical and subcortical regions have been noted in the CNS of HIV-infected individuals, with the extent of neurodegeneration in several brain regions (characterized by the loss of microtubule-associated protein 2 and synaptophysin) predicting global neuropsychological impairment ≤18 months prior to death [36]. In

Correspondence to: Mark A. Prendergast, prender@email.uky.edu.

particular, the hippocampus has been reported to be particularly susceptible to HIV-related neuroinflammation (reviewed in Xu and Ikez [54].

Infiltration of HIV-1 into the brain occurs primarily via infected monocytes, which, along with microglia, are the primary CNS cell type infected with HIV-1. However, the virus is also able to infect astrocytes and enter the brain in CSF and/or blood across the blood brain barrier with the help of viral envelope proteins [9]. Damage to neurons is primarily an indirect consequence of the release of cytokines, excitatory amino acids, chemokines, transcription factors, and viral proteins, such as gp120 and the transactivator of transcription (Tat) protein [8]. Tat is an HIV-1 nuclear regulatory protein that functions to stabilize viral gene transcription, and its release from infected cells in the CNS is postulated to promote neuronal injury [21, 22]; reviewed in King et al. [27]. Tat-related neuronal injury occurs via several different mechanisms, including activation of NMDA receptors and altered Ca^{2+} homeostasis [12, 28, 41, 46]; altered mitochondrial membrane potential and accumulation of reactive oxygen species [28]; blockade of pro-survival LRP receptor ligands [29]; and changes in microtubule dynamics [6, 16, 17]; reviewed in Giacca [23]. Microtubule-associated targets of Tat may be particularly important in initiating apoptotic signaling cascades. Alterations in microtubule polymerization or depolymerization, particularly as it relates to mitotic spindle function, are associated with initiation of apoptosis mediated by pro-apoptotic Bcl-2 proteins such as Bim (for review, see [11].

Thus, the current studies examined the effects of exposure to recombinant HIV-1 Tat(1-86) on MAP-dependent and MAP-independent microtubule formation ex vivo. Studies employing rat organotypic hippocampal explants examined the time-dependent effects of exposure to recombinant HIV-1 Tat(1-86) on oxidative neuronal injury and MAP-2 immunoreactivity in pyramidal cell layers of the CA1 and CA3 hippocampal regions, as well as, the granule cell layer of the dentate gyrus.

Experimental Procedures

Preparation of Recombinant HIV-1 Tat(1-86)

Recombinant Tat(1-86) was prepared as previously described [30]. Briefly, the tat gene encoding the 86 amino acid variant (first and second exons) was amplified from HIVBRU obtained from Dr. Richard Gaynor through the AIDS repository at the NIH and inserted into an E. coli vector PinPoint Xa2 (Promega, Madison, WI). Tat(1-86) was expressed as fusion proteins with naturally biotinylated protein at the N-terminus, and were purified on a column of soft release avidin resin, cleaved (using factor Xa), and eluted from the column followed by desalting with a PD10 column. To prevent oxidation of the proteins, all purification steps contained dithiothreitol. Purity of the Tat(1-86) proteins was found to be>95% by SDS–PAGE, and HPLC analysis using a C4 column displayed a single symmetrical peak. Functional activity of Tat(1-86) was confirmed using a transactivation assay in HL3T1 cells containing HIV-1 LTR-CAT construct [30]. Using a Pyrochrome Chromogenic test kit (Associates of Cape Cod, Falmouth, MA), the tat preparation was found to contain<1 pg/ml endotoxin. The proteins were then stored in a lyophilized form at −80°C in endotoxin-free siliconized microcentrifuge tubes until experiments were initiated. Single aliquots were used for each experiment due to the susceptibility of Tat(1-86) to degradation and loss of biological activity with each freeze–thaw cycle.

MAP-Independent and –Dependent Polymerization of Bovine Brain Tubulin

Formation of microtubules ex vivo was assessed by allowing for polymerization of purified bovine tubulin (at a concentration of 2 mg/ml) employing a turbidity assay in 96-well plate format (HTS-Tubulin Polymerization Assay Kit; Cytoskeleton, Denver, CO, USA). Initial

studies were conducted to confirm the sensitivity of the bovine brain tubulin polymerization assay to the inhibitory effects of a known polymerization inhibitor, the vinca alkaloid vincristine sulfate, derived from *Catharanthus roseus*. Vincristine sulfate binds to *αβ*-tubulin dimers to prevent formation of microtubules, thus leading to mitotic arrest and apoptosis (for review, see [26, 51]. Previous work has demonstrated the sensitivity of this assay to enhancement of microtubule formation with paclitaxel, which is an antineoplastic agent that promotes tubulin polymerization [42]. Polymerization of purified bovine brain tubulin was assessed both in the presence and absence of vincristine sulfate (0.1–10 μM; Sigma–Aldrich, St. Louis, MO). Absorption at 340 nm was measured every 5 min for 45 min using a Beckman-Coulter DTX 880 Multimodal Detector plate reader (Beckman-Coulter, Fullerton, CA, USA). The kinetic assay was terminated at 45 min, as microtubule polymerization has been observed to plateau and remain stable at all timepoints thereafter [42]. General tubulin buffer (G-PEM; Cytoskeleton) was used as a control measure of background absorbance.

Subsequent studies measured MAP-independent and MAP-dependent microtubule formation (polymerization of purified bovine brain tubulin) in the same turbidity assay, both in the presence and absence of recombinant HIV-1 Tat(1-86) (1–100 nM). This form of Tat has not previously been examined with regard to effects on microtubule formation or stabilization. The Tat(1-86) variant represents the most common amino acid form of the Tat protein detected in HIV-1 infections in the North America, and contains the amino acid sequence that appears necessary for Tat-induced cytotoxicity [38]. MAP-deficient tubulin (Cytoskeleton) was reconstituted with G-PEM buffer and placed into a pre-warmed 96-well plate (37°C). Varying concentrations of Tat(1-86) (1–100 nM) were added to separate wells containing reconstituted tubulin. In an additional set of experiments, Tat(1-86) (1–100 nM) was exposed in G-PEM buffer to bovine brain tubulin containing pre-bound MAPs (1 mg/ml; MAP-rich tubulin; Cytoskeleton). These concentrations of Tat(1-86) were chosen because they have been shown to decrease viability of hippocampal neurons in vitro, as measured by propidium iodide uptake [45]. Absorption at 340 nm was measured every 5 min for 45 min using a Beckman-Coulter DTX 880 Multimodal Detector plate reader, as described above.

Organotypic Hippocampal Slice Culture Preparation

Organotypic hippocampal slice cultures were prepared to assess time-dependent effects of Tat(1-86) on cell injury and/or death and MAP2(a,b) immunoreactivity. Eight-day old male and female Sprague–Dawley rat pups (Harlan Laboratories, Indianapolis, IN, USA) were humanely euthanized for aseptic whole brain removal. Brains were immediately transferred into frozen dissecting medium made of Minimum Essential Medium containing Hanks' salts and L-glutamine (MEM; Gibco, Gaithersburg, MD, USA), 25 mM HEPES (Sigma–Aldrich Co., St. Louis, MO, USA), and 50 μM Penicillin/Streptomycin (Gibco). Bilateral hippocampi were removed, cleaned of extra tissue under a dissecting microscope, and placed into chilled culture medium, which is composed of dissecting medium with the addition of: 36 mM glucose (Fisher Scientific, USA), 25% (v/v) Hanks' balanced salt solution (Gibco), 25% heat-inactivated horse serum (Sigma–Aldrich Co.), and 0.05% Penicillin/Streptomycin. Hippocampi were then sectioned coronally at 200 μm using the McIllwain Tissue Chopper (Mickle Laboratory Engineering Co. Ltd., Gomshall, UK) and placed into fresh culture medium. Morphologically intact slices were selected under a dissecting microscope and placed onto porous Teflon membrane inserts (Millicell-CM 0.4 μm; Millipore, Marlborough, MA). Inserts were pre-incubated in 35 mm 6-well culture plates with 1 ml of culture medium beneath the insert and placed into an incubator environment of 37°C, 5% CO_2/95% air. Three slices were placed onto each insert, yielding 18 slices per plate. Excess medium from the top of the membrane insert was aspirated. Slices were allowed five days in vitro (DIV) to attach to the insert membrane before any

experiments were conducted. This method was adapted from Stoppini et al. [48]. Care of animals was carried out in accordance with the National Institutes of Health Guide for the Care and Use of Laboratory Animals (NIH Publications No. 80-23, revised 1996), as well as the University of Kentucky's Institutional Animal Care and Use Committee. All experiments discussed below were replicated using different rat litters.

Propidium Iodide Uptake

Hippocampal cultures were exposed to recombinant Tat(1-86) (100 nM) in culture medium for 24, 72, or 120 h. Propidium iodide (PI; 3.74 μM) was present in the culture medium at the initiation of Tat(1-86) exposure for visualization of cell injury at their respective timepoints. To allow the cultures maximal exposure to the Tat(1-86) protein, one ml of culture medium containing Tat(1-86) and PI was slowly added to the top of the membrane insert and allowed to slowly diffuse through the porous membrane over the treatment period. A subset of cultures were co-exposed to Tat(1-86) and the anti-oxidant Trolox (500 μM) for 24, 72 or 120 h. This concentration of Trolox has previously shown neuroprotection in vitro in both organotypic cerebellar and hippocampal neurons [34, 37]. Cellular uptake of PI was visualized using fluorescent microscopy, and images were taken for future analysis. Images were taken using SPOT Advanced version 4.0.9 software for Windows (W. Nuhsbaum Inc., McHenry, IL, USA) with a 5× objective on an inverted Leica DMIRB microscope (W. Nuhsbaum Inc.) fitted for fluorescence detection (mercury-arc lamp) and connected to a personal computer via a SPOT 7.2 color mosaic camera (W. Nuhsbaum Inc.). PI has a maximum excitation wavelength of 536 nm and was excited using a band-pass filter that excites wavelengths between 515 and 560 nm. The emission of PI in the visual range is 620 nm. PI uptake, as measured by fluorescent intensity, was measured in the primary cell layers of the CA1, CA3, and DG hippocampal regions. NIH Image J software was used for densitometric analysis of fluorescent intensity in each hippocampal region, and fluorescent values from experimental groups were converted to percent control values before statistical analysis to reflect PI uptake relative to baseline cell death. N = mean of 56 fluorescent measurements for each hippocampal region.

MAP-2 Immunofluorescence

In separate cultures, immunoreactivity of microtubule associated protein-2 (MAP-2a,b), was measured in the primary cell layers of the CA1, CA3, and DG hippocampal regions after 24, 72, or 120 h exposure to Tat(1-86) (100 nM), with or without the addition of Trolox (500 μM) to the cell culture medium. After their respective exposure timepoints, cultures were removed from culture medium for fixation with 10% formalin. Formalin was applied to the bottom and top of cultures for 30 min, followed by two washes with 1× PBS and storage at 4°C until immunohistochemistry was conducted. At the initiation of the immunohistochemistry procedure, cultures were placed into a PBS buffer containing 0.005% bovine serum albumin and 0.1% Triton-X (Sigma–Aldrich) for 45 min to permeabilize cell membranes. Following this incubation period, cultures were transferred into fresh culture plates with 1 ml of 1× PBS on the bottom of the plate, and 1 ml of buffer containing a mouse anti-MAP-2a,b (Sigma–Aldrich; St. Louis MO, USA) monoclonal primary antibody was added slowly to the top of the culture membrane. Following 24 h incubation with primary antibody for MAP-2a,b at 4°C, OHSCs were washed twice in 1× PBS and placed into fresh culture plates with 1 ml of 1× PBS on the bottom of the plate, and 1 ml of buffer containing fluorescein isothiocynate (FITC)-conjugated secondary antibody (Sigma; 1:200; produced in mouse) was slowly added to the top of the culture membrane. After plates were incubated with secondary antibody at 4°C for 24 h, cultures were washed twice in 1× PBS and fluorescent images were taken. FITC fluorescence was elicited using a band-pass filter that excites wavelengths of approximately 495 nm (emission wavelength =

520 nm), and images were taken as described above. N = mean of 25 fluorescent measurements for each hippocampal region.

Data Analysis

For turbidity studies, light absorbance was measured at 340 nm every 5 min for a 45 minute period. Two-way repeated measures analyses were conducted (treatment group × timepoint) to determine effects of vincristine sulfate or Tat(1-86) on microtubule polymerization with or without MAPs. Holm-Sidak post-hoc tests were interpreted when appropriate. For analysis of PI uptake and MAP-2 immunoreactivity after Tat(1-86) and/or trolox exposure, images were analyzed using densitometry for the granule cell layer of the dentate gyrus and the pyramidal cell layers of the cornu ammonis (CA) 1 and 3 regions. Optical intensity measurements were converted to percent control before statistical analysis. For PI and MAP-2 studies, a two-way ANOVA (treatment × time) was conducted within each hippocampal region. Fishers LSD post-hoc tests were interpreted when appropriate. All experiments were replicated in triplicate.

Results

Effects of Vincristine Sulfate Exposure on Tubulin Polymerization

Initial studies were conducted to confirm the sensitivity of the tubulin polymerization assay to inhibition by exposure to a known inhibitor of polymerization, the vinca alkaloid vincristine sulfate (0.1–10 μM). Baseline absorbance measurements are indicated by absorbance of G-PEM buffer, which remained stable throughout the timepoints. A two-way repeated measures ANOVA indicated a significant treatment × cycle interaction ($F(24,107) = 43.933$, $P<0.001$), with tubulin polymerization inhibited by vincristine sulfate exposure in a time and concentration-dependent manner (Fig. 1). Nearly complete inhibition of tubulin polymerization was noted with exposure to 10 μM vincristine sulfate, while polymerization was reduced by approximately 50% at each time point of measurement with exposure to 0.1 μM vincristine sulfate (post hoc, $P<0.05$). Inhibition with exposure to 10 μM vincristine sulfate was not significantly greater than inhibition with exposure to 0.1 μM vincristine sulfate for the first 10 min of the assay, but was at each time point thereafter (Ps<0.05).

Effects of Tat(1-86) on MAP-Independent and MAP-Dependent Tubulin Polymerization

Additional studies examined tubulin polymerization in the presence or absence of Tat(1-86) (1–100 nM). Baseline absorbance measurements are indicated by absorbance of G-PEM buffer, which remained stable throughout the timepoints. A two-way repeated measures ANOVA (treatment × cycle) indicated a main effect of treatment ($P<0.001$) and a main effect of cycle ($P<0.01$). In regard to the main effect of treatment, tubulin polymerization was significantly inhibited by co-exposure to all concentrations of Tat(1-86) (Ps<0.01). Further, co-incubation of tubulin and Tat(1-86) resulted in absorbance measurements that were not different from control (G-PEM buffer). For the main effect of cycle on tubulin polymerization, irrespective of treatment, absorbance was significantly elevated during the last 5 min of the assay (cycle 9) as compared to the first 5 min of the assay (cycle 1; $P<0.01$; Fig. 2).

Before examining the effect of Tat(1-86) (1–100 nM) on polymerization of tubulin prepared with pre-bound MAPs (MAP-rich tubulin), a two-way ANOVA was conducted to compare polymerization of tubulin without MAPs (MAP-deficient tubulin; 2 mg/ml as used in above studies) with polymerization of MAP-rich tubulin. The two-way (treatment × cycle) ANOVA revealed that the presence of MAPs significantly increased tubulin polymerization at all timepoints ($P<0.05$; Fig. 3a). Subsequent studies examined the effect of Tat(1-86) (1–100 nM) on MAP-rich tubulin. A two-way repeated measures ANOVA revealed a treatment

× cycle interaction (P<0.001), indicating a concentration-dependent effect of Tat(1-86) on polymerization of MAP-rich tubulin (Fig. 3b). After 5 min of Tat(1-86) incubation with MAP-rich tubulin, the two highest concentrations of Tat(1-86) (10 and 100 nM) significantly reduced MAP-rich tubulin polymerization (Ps<0.01). The inhibition of MAP-rich tubulin polymerization by Tat(1-86) (10 and 100 nM) persisted for 25 min, at which point all Tat(1-86) concentrations (1–100 nM) were effective at blocking MAP-rich tubulin polymerization (Ps<0.01); an effect that persisted for the remainder of the kinetic assay (45 min).

Effects of Trolox and Tat(1-86) Co-Exposure on Neuronal Viability

As effects of Tat(1-86) exposure in the previous studies were not clearly concentration-dependent, organotypic hippocampal slice cultures were exposed to the middle concentration of Tat(1-86) that was used (100 nM) for 24, 72, or 120 h. A subset of cultures exposed to Tat(1-86) (100 nM) were also co-exposed to the soluble vitamin E analog Trolox (500 μM) or to Trolox alone. A two-way ANOVA (treatment × time) was conducted within each hippocampal region. Cell injury was observed in the granule cell layer of the DG, as indicated by a significant treatment × time interaction (F(6,315) = 4.512; P<0.001). In the DG, Tat(1-86) produced an approximately 30–35% increase in PI uptake above control values after 24 or 72 h exposure (Fisher's LSD, Ps<0.001), though increased PI uptake was no longer observed after 120 h of Tat(1-86) exposure. Co-exposure to Trolox significantly reduced the increase in PI uptake produced by Tat(1-86) exposure in the DG after 24 and 72 h of exposure (Fisher's LSD, Ps<0.001) (Fig. 4). Trolox alone did not alter PI uptake after 24 or 72 h of exposure, though 120 h of exposure to Trolox slightly, but significantly, resulted in less PI uptake as compared to control cultures in theDG(data not shown). In contrast to the DG, PI uptake was not altered by Tat(1-86) and/or trolox exposure in the CA3 or CA1 hippocampal regions at any timepoint (data not shown).

Effects of Trolox and Tat(1-86) Co-Exposure on MAP-2 Immunoreactivity

MAP-2(a,b) immunoreactivity was measured in organotypic hippocampal cultures after 24, 72, or 120 h exposure to Tat(1-86; 100 nM), Tat(1-86) and Trolox (500 μM) or Trolox alone. A two-way ANOVA (treatment × time) was conducted within each hippocampal region. Within the DG, there was a significant main effect of treatment (F(3,107) = 1.696), such that Tat(1-86) exposure resulted in a significant reduction in MAP-2 immunoreactivity compared to control cultures (Fisher's LSD, P<0.05). However, Tat(1-86)-induced decreases in MAP-2 immunoreactivity were entirely reversed with concurrent exposure to Trolox (Fisher's LSD, P<0.001). Similarly, a main effect of treatment was also present within the CA1 region and the CA3 region, such that Tat(1-86) exposure resulted in a significant reduction in MAP-2 immunoreactivity (Fisher's LSD, CA1: P<0.05; CA3: P<0.001). As in the DG, the reduction in MAP-2 in the CA1 and CA3 regions are also reversed with Trolox exposure (Fig. 5). Trolox alone did not affect MAP-2(a,b) immunoreactivity in any hippocampal region at any timepoint (data not shown). Representative images of PI uptake and MAP-2(a,b) immunoreactivity in organotypic hippocampal slices exposed to Tat(1-86) and Tat(1-86) + Trolox are presented in Fig. 6.

Discussion

A significant portion of individuals affected by HIV-1 develop symptoms of neurodegeneration and neurocognitive impairment [25]. The HIV transcription factor Tat directly and indirectly promotes neuronal death in vitro, though it is unclear if different Tat variants influence the same or different neuronal substrates to produce neuronal injury. The use of several distinct native or recombinant Tat variants has previously been reported to have varying effects on cytoskeletal proteins, including enhancement of microtubule

polymerization or stabilization of microtubules via direct binding to tubulin [17]; direct interaction with microtubule-associated proteins (MAPs); or indirect promotion of microtubule destruction by inducing proteasomal translocation to microtubules [6]. Disruption of microtubule dynamics and activation of Bcl-2 protein-mediated pro-apoptotic signaling have been postulated to be important mediators of Tat-induced cytotoxicity (for review, see [23]. However, a consistent effect of different Tat variants on microtubule dynamics has not been clearly established, though the Tat(31-61) epitope appears necessary for Tat-related increases in intracellular Ca^{2+} and toxicity [38, 46]; suggesting that some similarities should exist in neurotoxic response to exposure to many Tat variants that have been studied.

The current data demonstrate reduced tubulin polymerization in the presence or absence of MAPs with exposure to recombinant Tat(1-86), suggesting that this variant of Tat directly interacts with tubulin dimers with high affinity at a site(s) distinct from those bound by MAPs. Microtubule- associated proteins, including MAP-2, tau, and LIS-1, among others, function to stabilize and promote microtubule assembly by cross-linking associated tubulin dimers [18]. However, the presence of such proteins (i.e. with use of MAP-rich tubulin preparations) in the current tubulin preparation did not alter the ability of Tat(1-86) to impair polymerization. It should be noted, however, that these are the first findings examining the effects of recombinant Tat(1-86) on microtubule dynamics, and these effects were demonstrated using nanomolar concentrations. That being said, previous studies of the effect of different Tat variants on tubulin polymerization have elicited varying results; perhaps in part due to differences in the Tat variant used; the cell type being studied; or the marker of interest being measured in response to Tat exposure. For example, exposure to wild-type Tat prevents microtubule depolymerization by binding to α- and β-tubulin dimers at a MAP-independent site in human 293T-cells, as it was shown that wild-type Tat interacts with both free tubulin dimers and polymerized microtubules [16]. In a turbidity assay, exposure of lamb brain-derived tubulin to the holo-Tat variant has also been shown to promote microtubule polymerization, though much higher concentrations (μM range) were used compared to the current study [19]. The holo-Tat variant differs from wild-type Tat near the cysteine- rich region of the protein sequence. Interestingly, Mishra et al. [33] reported that the neurotoxicity associated with exposure to the wild-type Tat protein of HIV-1 virus Clade B (the form most prevalent in North American and Europe) in cultured human fetal neurons is dependent on the existence of the dicysteine C30C31 motif, suggesting that different mechanisms of cell death may be initiated by different Tat variants.

The sensitivity of the tubulin polymerization assay employed to both the inhibitory effects on polymerization by vincristine sulfate and promoting effects on polymerization by paclitaxel support its use in the study of microtubule dynamics [42]. Though it is unclear why the inhibition of microtubule polymerization with Tat(1-86) was not concentration-dependent, a similar lack of concentration dependent apoptosis in neurons has been reported with exposure to Tat [28], thus suggesting that a greater range of Tat concentrations would be beneficial for capturing the entire scope of effects produced by each Tat variant on multiple measures of cellular integrity. However, similar to the current studies, other laboratories have also not found facilitation of microtubule polymerization. For instance, it has been reported that exposure to 100 μM recombinant Tat(1-72) delays polymerization of porcine brain tubulin, and the authors suggest this occurs by competition for MAP-binding sites [10]. The interpretation of the findings by Battaglia et al. [10] are supported by findings that Tat(1-72) co-immunoprecipitated with the MAP LIS1 in Tat-transfected HeLa cells [20]. Conversely, exposure of lamb brain-derived tubulin has shown facilitation of MAP-independent tubulin polymerization with exposure to the variant Tat (38-72) [17]. Thus, it is quite clear that distinct variants of HIV-1 Tat have divergent effects on microtubule

dynamics, including both direct interactions with MAP-sensitive domains on α/β-tubulin dimers and effects at MAP-insensitive domains.

Several Tat variants have direct protein–protein interactions with tubulin dimers and/or MAPs that alter microtubule integrity and likely compromise neuronal viability. This is demonstrated by the present findings with regard to Tat(1-86) effects on tubulin polymerization, as well as other preparations employing purified tubulin [16, 17] and evidence that Tat(1-72) co-immunoprecipitates with LIS-1 [20]. It has also been shown that exposure to Tat variants affect the integrity of cytoskeletal proteins by initiation of oxidative stress mechanisms. This possibility may be important given evidence that serum of HIV-1 positive individuals is characterized by decreased glutathione levels, and increased lipid peroxidation and DNA fragmentation in leukocytes [24], with brain tissue from HIV-1 positive individuals showing increased concentrations of protein carbonyl formation [50]. Additionally, exposure of non-neuronal HeLa cells stably expressing the Tat gene for Tat(1-86), but not Tat(1-72), was associated with reduced levels of the anti-oxidant defense enzyme Mn-dependent superoxide dismutase [52]. Further, Price et al. [43] demonstrated that exposure of endothelial cells to full-length Tat was associated with markers of oxidative stress, including reductions in intracellular glutathione and elevations in malondialdehyde. In microglia, Bruce-Keller et al. [13] reported that exposure to recombinant Tat(1-72) elevated multiple markers of oxidative stress. Similar to the current data, Aksenov et al. [3] demonstrated in dissociated fetal rat hippocampal cell cultures that prolonged exposure to recombinant Tat(1-72) increased production of reactive oxygen species and promoted apoptotic-like cytotoxicity; effects that were reduced with co-exposure to Trolox. The current data showing that neuroprotection by Trolox against Tat-induced cytotoxicity and the literature cited above suggest that multiple variants of Tat contribute to cellular damage related to oxidative stress.

Though much evidence exists for direct interactions of Tat with tubulin dimers and/or MAPs to promote cell death, the initiation of oxidative stress pathways also contributes to neuronal injury interaction with cytoskeletal proteins. One consequence of oxidative stress, lipid peroxidation, results in byproducts that interact with cytoskeletal proteins and decrease cellular viability. Specifically in neuronal tissue, oxidative stress byproducts increase phosphorylation and prevent dephosphorylation of the MAP tau in cultured rat hippocampi [32]; disrupt formation of microtubules in neuroblastoma cells, leading to stunted neurite growth due to direct interactions with α and β tubulin proteins [39]; decrease abundance of proteins integral to cytoskeleton maintenance, including microfilaments, microtubules, and vimentin, independent of changes in gene expression [5]; and cross-link cytoskeletal proteins and adduct formation in P19 neuroglial cultures [35]. Thus, Tat contributes to microtubule destruction via direct interactions on tubulin dimers and initiation of oxidative stress pathways.

In the current studies, Tat(1-86) exposure produced significant cytotoxicity in the granule cells of the dentate gyrus. Injury with exposure to recombinant Tat(1-86) was not unexpected, as Tat(1-86) has been widely reported to produce apoptotic neuronal injury in the developing brain [1, 2, 12]. Importantly, the anti-oxidant Trolox attenuated Tat(1-86)-induced injury in the dentate gyrus, and also MAP-2 loss in granule cells of the dentate gyrus and pyramidal cells of the CA3 and CA1 regions. Trolox has also been shown to prevent decreases in mitochondrial potential in cultured human fetal neurons exposed to CSF from HIV-1 positive individuals, which correlated in vitro with increased cytochrome c release and apoptosis [50]. The present findings are the first to suggest oxidative stress as a mechanism injury with exposure to the Tat(1-86) variant, which is in accordance with studies that have shown Tat(1-72) to induce oxidative stress in various cell preparations, including brain microvascular endothelial cells, striatal neurons, and primary hippocampal

cultures [3, 4, 49]. These findings also extend previous work in demonstrating greater vulnerability of the DG to cell injury with exposure to Tat(1-86), suggesting hippocampal region-specific effects of recombinant Tat(1-86) [45]. The present data go further, however, in indicating that the granule cells of the dentate gyrus are more vulnerable to oxidative injury with exposure to Tat(1-86), though increased PI uptake after Tat exposure was absent by 120 h. This effect may suggest the presence of phagocytic activity and resulting loss of DNA available for PI to bind. PI fluoresces upon excitation after binding to DNA; however, PI is membrane impermeant, thus it is only able to enter the intracellular compartment and bind DNA in damaged or dead cells, and is generally accepted as a marker of cell injury/death [40]. A more thorough time-course of Tat(1-86)-related injury in the current model could be helpful in understanding when and if cellular death measured by PI uptake directly corresponds to reduced MAP-2 immunofluorescence, and perhaps loss of cytoskeletal integrity.

Though organotypic hippocampal studies of cell death have shown the greatest damage in response to Tat(1-86) in the DG, in vivo administration of Tat(1-72) in rodents is characterized by more extensive hippocampal injury, such that dentate gyrus and CA3 regions demonstrate reduced synaptophysin levels, increased lesion volume, increased GFAP immunoreactivity [14], reduced cell viability, and reduced MAP-2 immunoreactivity [31]. This is in keeping with neuronal insult in human post-mortem tissue from HIV-1 infected individuals, such that reduced MAP-2 immunoreactivity has been observed in the dentate gyrus [31], and reduced dendritic branching has been noted in dentate gyrus and CA3 regions [44]. Previous work has shown endocytosis of Tat protein in the DG when administered in vivo, and subsequent migration down mossy fiber pathways to the CA3 to produce neurotoxicity [15], conferring more extensive hippocampal injury in in vivo models compared to in vitro models. However, the current data demonstrate MAP-2 loss in CA3 and CA1 hippocampal regions in addition to the DG, though significant cell injury was not observed in these regions at the time-points observed. MAP-2 loss in pyramidal CA region neurons in human HIV-1 positive individuals correlates with overall reduced hippocampal volume [7], though it is unclear whether increased cell death within a hippocampal region always occurs in tandem with MAP-2 loss. For example, dendritic pruning that occurs in Drosophila-derived neurons involves activation of caspases that are unique to the dendrites, not the soma or axon, suggesting that cell injury and MAP-2 loss may follow distinct time-courses and regional specificity [53].

In sum, the present data demonstrate that recombinant Tat(1-86) impairs microtubule formation by interacting with tubulin dimers at a site(s) distinct from that associated with MAP-potentiation of microtubule formation. Further, studies of intact organotypic hippocampal explants demonstrated alleviation of Tat-associated cell injury by use of an anti-oxidant, suggesting the importance of oxidative stress in Tat(1-86)-related damage. These findings support the hypothesis that microtubules and microtubule associated proteins are targets of Tat(1-86) in the development of oxidative stress-associated neurodegeneration.

Acknowledgments

The authors acknowledge the support of AA013561.

References

1. Adams SM, Aksenova MV, Aksenov MY, et al. ER-beta mediates 17 beta-estradiol attenuation of HIV-1 Tat-induced apoptotic signaling. Synapse. 2010; 64(11):829–838. [PubMed: 20340172]

2. Aksenov MY, Aksenov MV, Mactutus CF, et al. Attenuated neurotoxicity of the transactivation-defective HIV-1 Tat protein in hippocampal cultures. Exp Neurol. 2009; 219:586–590. [PubMed: 19615365]
3. Aksenov MY, Aksenova MV, Nath A, et al. Cocaine-mediated enhancement of Tat toxicity in rat hippocampal cell cultures: The role of oxidative stress and D1 dopamine receptor. Neurotoxicology. 2006; 27:217–228. [PubMed: 16386305]
4. Aksenov MY, Hasselrot U, Wu G, et al. Temporal relationships between HIV-1 Tat induced neuronal degeneration, OX-42 immunoreactivity, reactive astrocytosis, and protein oxidation in the rat striatum. Brain Res. 2003; 987(1):1–9. [PubMed: 14499939]
5. Allani PK, Sum T, Bhansali SG, et al. Comparative study of the effect of oxidative stress on the cytoskeleton in human cortical neurons. Toxicol Appl Pharmacol. 2004; 196:29–36. [PubMed: 15050405]
6. Aprea S, Del Valle L, Mameli G, et al. Tubulin-mediated binding of human immunodeficiency virus-1 Tat to the cytoskeleton causes proteasomal-dependent degradation of microtubule-associated protein 2 and neuronal damage. J Neurosci. 2006; 26:4054–4062. [PubMed: 16611822]
7. Archibald SL, Masliah E, Fennema-Notestine C, et al. Correlation of in vivo neuroimaging abnormalities with postmortem human immunodeficiency virus encephalitis and dendritic loss. Arch Neurol. 2004; 61:369–376. [PubMed: 15023814]
8. Banks WA, Robinson SM, Nath A. Permeability of the blood-brain barrier to HIV-1 Tat. Exp Neurol. 2005; 193:218–227. [PubMed: 15817280]
9. Banks WA, Freed EO, Wolf KM, et al. Transport of human immunodeficiency virus type 1 pseudoviruses across the blood–brain barrier: role of envelope proteins and adsorptive endocytosis. J Virol. 2001; 75:4681–4691. [PubMed: 11312339]
10. Battaglia PA, Zito S, Macchini A, et al. A Drosophila model of HIV-Tat related pathogenicity. J Cell Sci. 2001; 114(Pt 15):2787–2794. [PubMed: 11683412]
11. Bhalla KN. Microtubule-targeted anticancer agents and apoptosis. Oncogene. 2003; 22:9075–9086. [PubMed: 14663486]
12. Bonavia R, Bajetto A, Barbero S, et al. HIV-1 Tat causes apoptotic death and calcium homeostasis alterations in rat neurons. Biochem Biophys Res Commun. 2001; 288:301–308. [PubMed: 11606043]
13. Bruce-Keller AJ, Barger SW, Moss NI, et al. Pro-inflammatory and pro-oxidant properties of the HIV protein Tat in a microglial cell line: attenuation by 17 beta-estradiol. J Neurochem. 2001; 78:1315–1324. [PubMed: 11579140]
14. Bruce-Keller AJ, Chauhan A, Dimayuga FO, et al. Synaptic transport of human immunodeficiency virus-Tat protein causes neurotoxicity and gliosis in rat brain. J Neurosci. 2003; 23:8417–8422. [PubMed: 12968004]
15. Chauhan A, Turchan J, Pocernich C, et al. Intracellular human immunodeficiency virus Tat expression in astrocytes promotes astrocyte survival but induces potent neurotoxicity at distant sites via axonal transport. J Biol Chem. 2003; 278:13512–13519. [PubMed: 12551932]
16. Chen D, Wang M, Zhou S, et al. HIV-1 Tat targets microtubules to induce apoptosis, a process promoted by the proapoptotic Bcl-2 relative Bim. EMBO J. 2002; 21:6801–6810. [PubMed: 12486001]
17. de Mareuil J, Carre M, Barbier P, et al. HIV-1 Tat protein enhances microtubule polymerization. Retrovirology. 2005; 2:5. [PubMed: 15691386]
18. Desai A, Mitchison TJ. Microtubule polymerization dynamics. Annu Rev Cell Dev Biol. 1997; 13:83–117. [PubMed: 9442869]
19. Egele C, Barbier P, Didier P, et al. Modulation of microtubule assembly by the HIV-1 Tat protein is strongly dependent on zinc binding to Tat. Retrovirology. 2008; 5:62. [PubMed: 18613978]
20. Epie N, Ammosova T, Sapir T, et al. HIV-1 Tat interacts with LIS1 protein. Retrovirology. 2005; 2:6. [PubMed: 15698475]
21. Eugenin EA, D'Aversa TG, Lopez L, et al. MCP-1 (CCL2) protects human neurons and astrocytes from NMDA or HIV-tat-induced apoptosis. J Neurochem. 2003; 85:1299–1311. [PubMed: 12753088]

22. Garcia-Martinez LF, Ivanov D, Gaynor RB. Association of Tat with purified HIV-1 and HIV-2 transcription preinitiation complexes. J Biol Chem. 1997; 272:6951–6958. [PubMed: 9054383]
23. Giacca M. HIV-1 Tat, apoptosis and the mitochondria: a tubulin link? Retrovirology. 2005; 2:7. [PubMed: 15698476]
24. Gil L, Martinez G, Gonzalez I, et al. Contribution to characterization of oxidative stress in HIV/AIDS patients. Pharmacol Res. 2003; 47:217–224. [PubMed: 12591017]
25. Gonzalez-Scarano F, Martin-Garcia J. The neuropathogenesis of AIDS. Nat Rev Immunol. 2005; 5:69–81. [PubMed: 15630430]
26. Jordan A, Hadfield JA, Lawrence NJ, et al. Tubulin as a target for anticancer drugs: agents which interact with the mitotic spindle. Med Res Rev. 1998; 18:259–296. [PubMed: 9664292]
27. King JE, Eugenin EA, Buckner CM, et al. HIV tat and neurotoxicity. Microbes Infect. 2006; 8:1347–1357. [PubMed: 16697675]
28. Kruman II, Nath A, Mattson MP. HIV-1 protein Tat induces apoptosis of hippocampal neurons by a mechanism involving caspase activation, calcium overload, and oxidative stress. Exp Neurol. 1998; 154:276–288. [PubMed: 9878167]
29. Liu Y, Jones M, Hingtgen CM, et al. Uptake of HIV-1 tat protein mediated by low-density lipoprotein receptor-related protein disrupts the neuronal metabolic balance of the receptor ligands. Nat Med. 2000; 6:1380–1387. [PubMed: 11100124]
30. Ma M, Nath A. Molecular determinants for cellular uptake of Tat protein of human immunodeficiency virus type 1 in brain cells. J Virol. 1997; 71:2495–2499. [PubMed: 9032389]
31. Maragos WF, Tillman P, Jones M, et al. Neuronal injury in hippocampus with human immunodeficiency virus transactivating protein, Tat. Neuroscience. 2003; 117:43–53. [PubMed: 12605891]
32. Mattson MP, Fu W, Waeq G, et al. Hydroxynonenal, a product of lipid peroxidation, inhibits dephosphorylation of the microtubule-associated protein tau. Neuroreport. 1997; 8:2275–2281. [PubMed: 9243625]
33. Mishra M, Vetrivel S, Siddappa NB, et al. Clade-specific differences in neurotoxicity of human immunodeficiency virus-1 B and C Tat of human neurons: Significance of dicysteine C30C31 motif. Ann Neurol. 2008; 63:366–376. [PubMed: 18074388]
34. Mizuhashi S, Ikegaya Y, Matsuki N. Cytotoxicity of tributyltin in rat hippocampal slice cultures. Neurosci Res. 2000; 38:35–42. [PubMed: 10997576]
35. Montine TJ, Amarnath V, Martin ME, et al. E-4-hydroxy-2- nonenal is cytotoxic and cross-links cytoskeletal proteins in P19 neuroglial cultures. Am J Pathol. 1996; 148:89–93. [PubMed: 8546230]
36. Moore DJ, Masliah E, Rippeth JD, et al. Cortical and subcortical neurodegeneration is associated with HIV neurocognitive impairment. AIDS. 2006; 20:879–887. [PubMed: 16549972]
37. Mulholland PJ, Stepanyan TD, Self RL, et al. Corticosterone and dexamethasone potentiate cytotoxicity associated with oxygen-glucose deprivation in organotypic cerebellar slice cultures. Neuroscience. 2005; 136:259–267. [PubMed: 16182452]
38. Nath A, Psooy K, Martin C, et al. Identification of a human immunodeficiency virus type 1 Tat epitope that is neuroexcitatory and neurotoxic. J Virol. 1996; 70:1475–1480. [PubMed: 8627665]
39. Neely MD, Sidell KR, Graham DG, et al. The lipid peroxidation product 4-hydroxynonenal inhibits neurite outgrowth, disrupts neuronal microtubules and modifies cellular tubulin. J Neurochem. 1999; 72:2323–2333. [PubMed: 10349841]
40. Noraberg J, Kristensen BW, Zimmer J. Markers for neuronal degeneration in organotypic slice cultures. Brain Res Protoc. 1999; 3:278–290.
41. Prendergast MA, Rogers DT, Mulholland PJ, et al. Neurotoxic effects of the human immunodeficiency virus type-1 transcription factor Tat require function of a polyamine sensitive-site on the N-methyl-D-aspartate receptor. Brain Res. 2002; 954:300–307. [PubMed: 12414113]
42. Prendergast MA, Self RL, Smith KJ, et al. Microtubule-associated targets in chlorpyrifos oxon hippocampal neurotoxicity. Neuroscience. 2007; 146:330–339. [PubMed: 17321052]
43. Price TO, Ercal N, Nakaoke R, et al. HIV-1 viral proteins gp120 and Tat induce oxidative stress in brain endothelial cells. Brain Res. 2005; 1045:57–63. [PubMed: 15910762]

44. Sa MJ, Madeira MD, Ruela C, et al. Dendritic changes in the hippocampal formation of AIDS patients: a quantitative Golgi study. Acta Neuropathol. 2004; 107:97–110. [PubMed: 14605830]
45. Self RL, Mulholland PJ, Harris BR, et al. Cytotoxic effects of exposure to the human immunodeficiency virus type 1 protein Tat in the hippocampus are enhanced by prior ethanol treatment. Alcohol Clin Exp Res. 2004; 28:1916–1924. [PubMed: 15608609]
46. Self RL, Mulholland PJ, Nath A, et al. The human immunodeficiency virus type-1 transcription factor Tat produces elevations in intracellular Ca2 + that require function of an N-methyl-D-aspartate receptor polyamine-sensitive site. Brain Res. 2004; 995:39–45. [PubMed: 14644469]
47. Singer EJ, Valdes-Sueiras M, Commins D, et al. Neurologic presentations of AIDS. Neurol Clin. 2010; 28:253–275. [PubMed: 19932385]
48. Stoppini L, Buchs PA, Muller D. A simple method for organotypic cultures in nervous tissue. J Neurosci Methods. 1991; 37:173–182. [PubMed: 1715499]
49. Toborek M, Lee YW, Pu H, et al. HIV-Tat protein induces oxidative and inflammatory pathways in brain endothelium. J Neurochem. 2003; 84(1):169–179. [PubMed: 12485413]
50. Turchan J, Pocernich CB, Gairola C, et al. Oxidative stress in HIV demented patients and protection ex vivo with novel antioxidants. Neurology. 2003; 60:307–314. [PubMed: 12552050]
51. Wang LG, Liu XM, Kreis W, et al. The effect of antimicrotubule agents on signal transduction pathways of apoptosis: a review. Cancer Chemother Pharmacol. 1999; 44:355–361. [PubMed: 10501907]
52. Westendorp MO, Shatrov VA, Schulze-Osthoff K, et al. HIV-1 Tat potentiates TNF-induced NF-kappa B activation and cytotoxicity by altering the cellular redox state. EMBO J. 1995; 14:546–554. [PubMed: 7859743]
53. Williams DW, Kondo S, Krzyzanowska A, et al. Local caspase acitivity directs engulfment of dendrites during pruning. Nat Neurosci. 2006; 9:1234–1236. [PubMed: 16980964]
54. Xu J, Ikez T. The comorbidity of HIV-associated neurocognitive disorders and Alzheimer's disease: a foreseeable medical challenge in post-HAART era. Neuroimmune Pharmacol. 2009; 4:200–212.

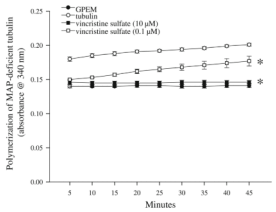

Fig. 1.

Exposure of purified bovine brain tubulin to the vinca alkaloid vincristine sulfate sulfate impairs tubulin polymerization in a concentration-dependent manner. Exposure to 0.1 or 10 μM vincristine sulfate reduced tubulin polymerization by 50–100% at each time point examined for 45 min, though inhibition of tubulin polymerization was significantly greater with exposure to 10 μM vincristine sulfate. *P<0.05 vs. tubulin for each concentration of vincristine at all timepoints measured

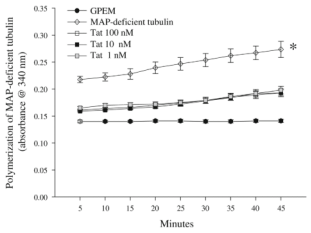

Fig. 2.

Exposure to recombinant Tat(1-86) (1–100 nM) impairs polymerization of purified bovine brain tubulin by 75–90% at each time point examined for 45 min. No differences between Tat(1-86) concentrations in inhibition of tubulin polymerization were noted. **P*<0.05 vs. all groups at all timepoints measured

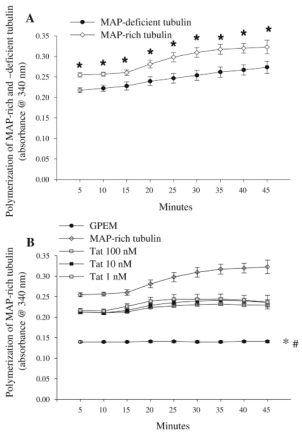

Fig. 3.

a The presence of pre-bound MAPs significantly increased polymerization of purified bovine brain tubulin at all timepoints measured; **P*s<0.05 vs. MAP-deficient tubulin. **b** Exposure to the two highest concentrations of Tat(1-86) (10 and 100 nM) impairs polymerization of MAP-rich bovine brain tubulin at every timepoint (*P*s<0.01), though all concentrations of Tat(1-86) (1–100 nM) impaired polymerization of MAP-rich bovine brain tubulin beginning at the 25 min timepoint. **a** **P*<0.05 vs. MAP-deficient tubulin; **b** **P*<0.01 vs. Tat(1-86) (10 and 100 nM) and MAP-rich tubulin for all timepoints; #*P*<0.01 vs. all concentrations of Tat(1-86) beginning at the 25 min timepoint and MAP-rich tubulin

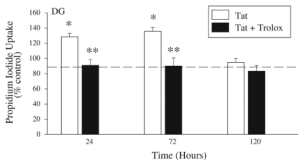

Fig. 4.

Prolonged exposure to recombinant Tat(1-86) (100 nM) produced significant cell death and/or injury in the granule cell layer of the dentate gyrus after 24 and 72 h of exposure, but not after 120 h of exposure. Co-exposure to Trolox (500 μM) significantly reduced PI uptake induced by Tat after 24 and 72 h exposure in organotypic hippocampal cultures. Exposure to Trolox alone resulted in slight, but significantly, less PI uptake than control in the DG at 120 h, but did not affect PI uptake compared to control in the CA3 or CA1 regions. The dashed line represents control values. *P<0.001 vs. control; **P<0.001 vs. Tat within each respective timepoint

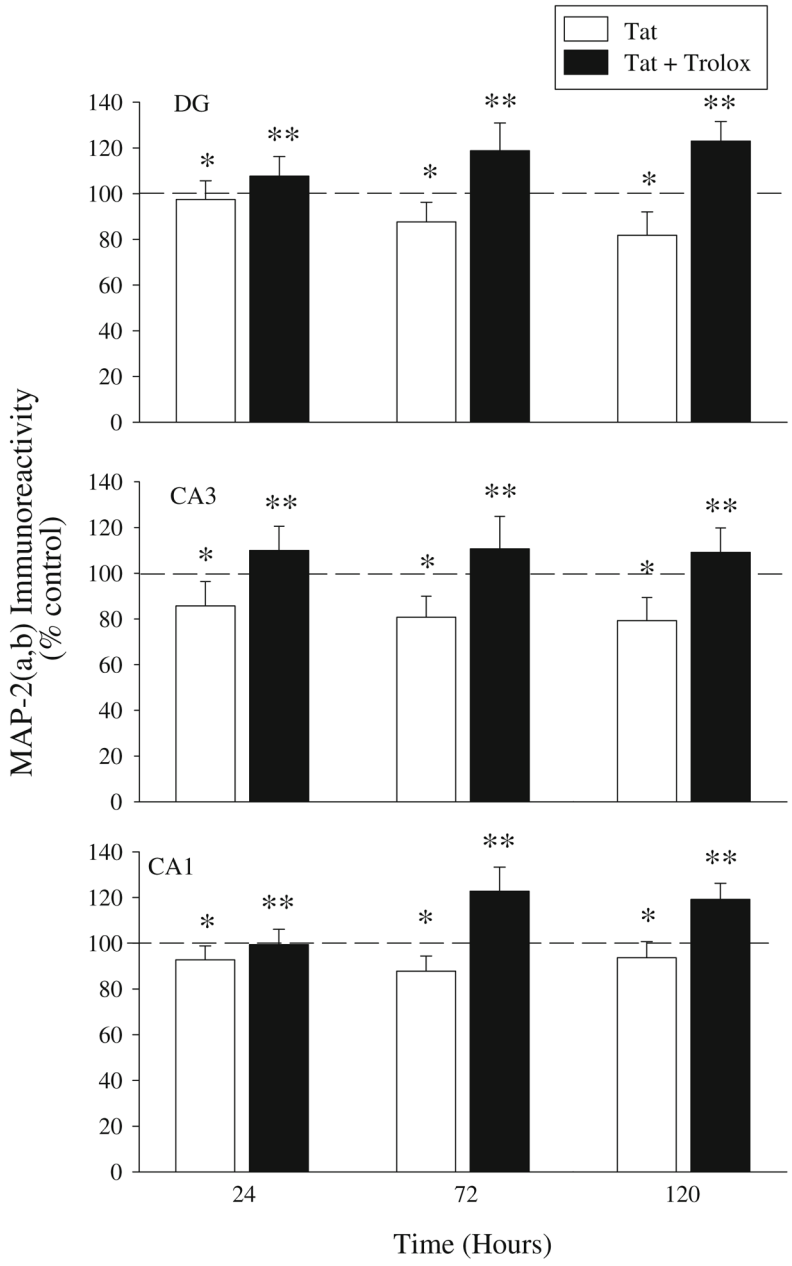

Fig. 5.

Exposure to recombinant Tat(1-86) (100 nM) produced significant loss of MAP-2(a,b) immunoreactivity in the granule cell layer of the dentate gyrus and pyramidal cell layers of the CA3 and CA1 regions, with no significant treatment × time interactions noted in any region. Co-exposure to Trolox (500 μM) significantly amelio-rated MAP-2(a,b) loss in organotypic hippocampal cultures. Trolox alone did not affect MAP-2(a,b) immunoreactivity in any hippocampal region at any timepoint. The dashed line represents control values. *P<0.001 vs. control; **P<0.001 vs. Tat

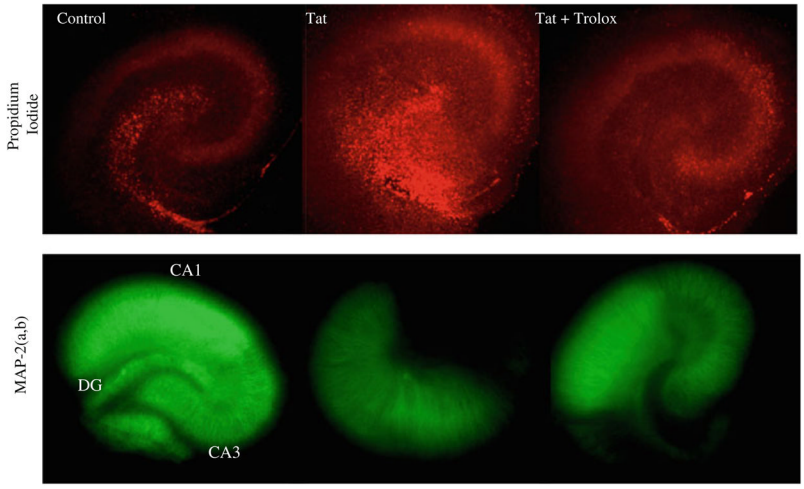

Fig. 6.

Representative images of PI uptake and MAP-2 immunofluorescence in control, Tat-exposed, and Tat + Trolox-exposed organotypic hippocampal cultures following 72 h exposure